

# Intermediate amplitude collective motion in $^{52}\text{Ti}$ with TDHFB

K. Sasakura and Y. Hashimoto,  
Graduate School of Pure and Applied Sciences  
Univ. of Tsukuba

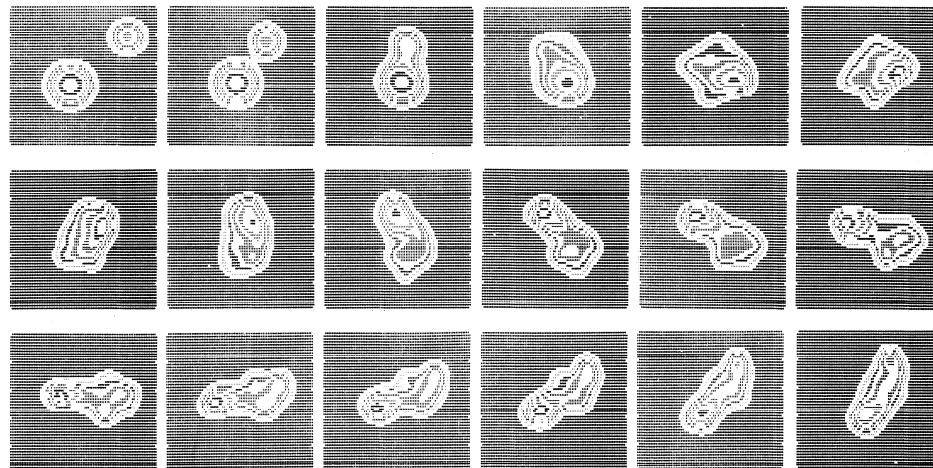
# Introduction

Time-dependent mean-field theories

Small amplitude → RPA, normal modes

Large amplitude

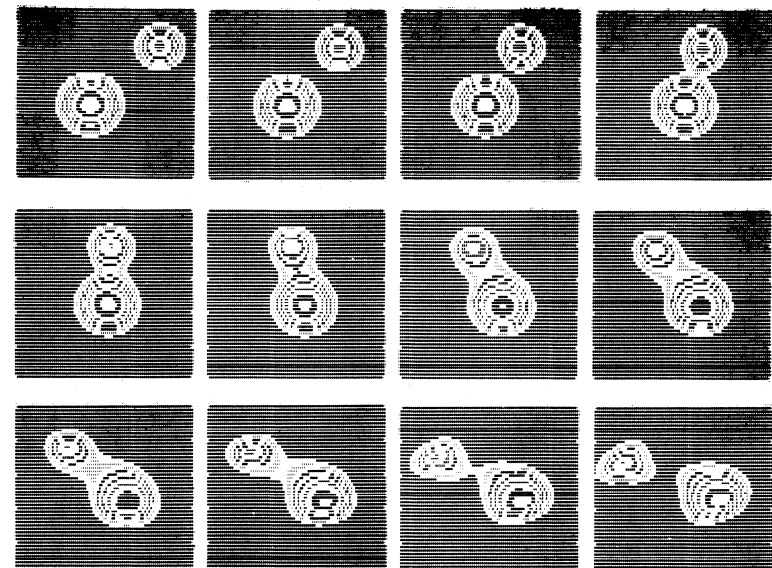
→ simulation of nuclear fusion and/or fission

FIG. 39. Contour plots for the same reaction as in Fig. 38 with an initial angular momentum of  $l=60\hbar$ .

energy transfer :  
relative motion  
→ internal collective/nucleonic motions

one-body dissipation  
(2 body collision neglected)

its mechanism ???  
← candidate : chaotic motion in TDHF (?)

FIG. 40. Contour plots for the same reaction as in Fig. 38 with an initial angular momentum of  $l=80\hbar$ .

## A Numerical Study on the Structure Change of Collective Motions

Yukio HASHIMOTO, Kazuo IWASAWA,\* Fumihiko SAKATA\* and Akio NARUI

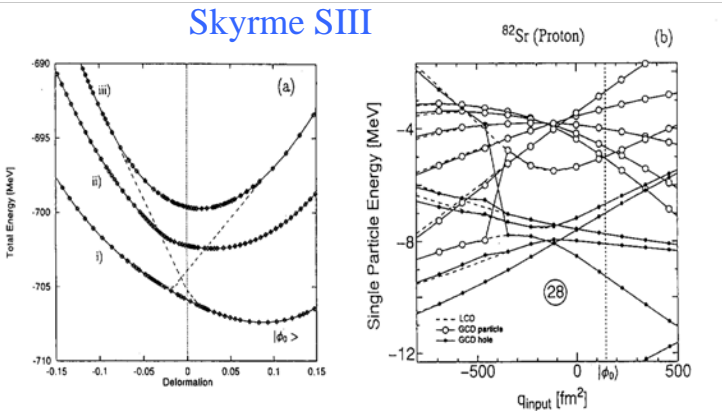


Fig. 1. (a) Continuous CHF lines. The lowest line i) passes through the ground state  $|\phi_0\rangle$ . The dense calculated points near  $q=0.02$  and  $q=-0.05$  indicate an abrupt character change occurring in line i). To illustrate “diabatic line” having no abrupt change, the dashed lines are drawn by hand. (b) The corresponding single-particle energy levels. Solid lines are results from the global configuration dictated (GCD) method, and dashed lines are from the local configuration dictated (LCD) method. The filled and open circles represent the occupied and unoccupied states, respectively. (Borrowed from Ref. 4).

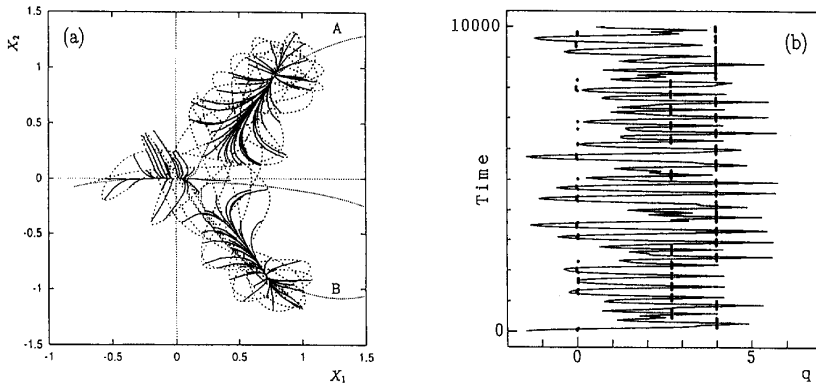


Fig. 8. (a) and (b) As in Fig. 6 but for the TDHF trajectory (dashed curve) in Fig. 5. The resulting points are  $\phi_0$ ,  $\phi_1$  and  $\phi_2$ .

three-level model

## BKN force

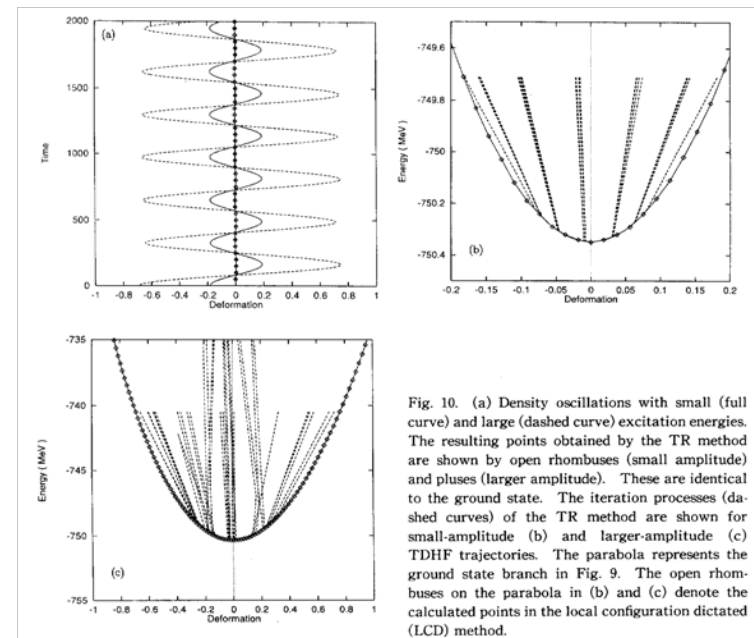
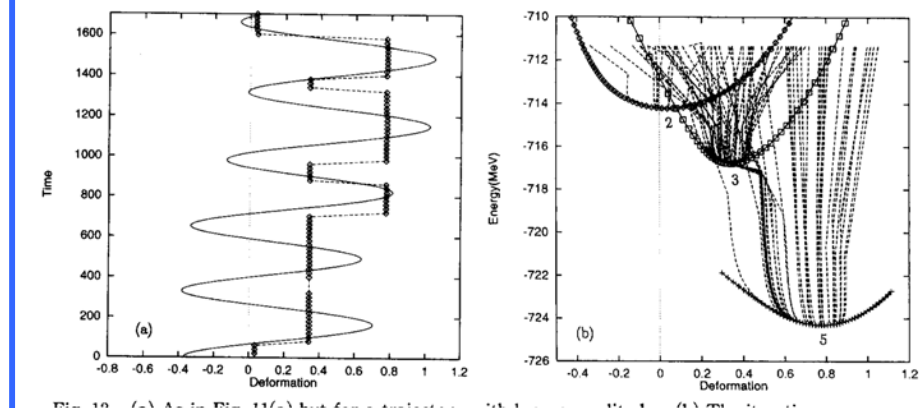


Fig. 10. (a) Density oscillations with small (full curve) and large (dashed curve) excitation energies. The resulting points obtained by the TR method are shown by open rhombuses (small amplitude) and pluses (larger amplitude). These are identical to the ground state. The iteration processes (dashed curves) of the TR method are shown for small-amplitude (b) and larger-amplitude (c) TDHF trajectories. The parabola represents the ground state branch in Fig. 9. The open rhombuses on the parabola in (b) and (c) denote the calculated points in the local configuration dictated (LCD) method.



# From TDHF to TDHFB

- ☆ make clear the role of pairing correlation  
in larger amplitude collective motion  
(within mean-field framework)
- ☆ invent tools to understand the microscopic  
(single-particle) dynamics

# Equations of motion of matrices $\mathbf{U}$ & $\mathbf{V}$

see Ring & Schuck

$$i\hbar \frac{\partial}{\partial t} \begin{pmatrix} U(t) \\ V(t) \end{pmatrix} = \mathcal{H} \begin{pmatrix} U(t) \\ V(t) \end{pmatrix}$$

$$i\hbar \frac{\partial}{\partial t} \mathcal{R} = [\mathcal{H}, \mathcal{R}],$$

$$\mathcal{H} = \begin{bmatrix} h_1 & \Delta \\ \Delta^\dagger & -h_1^* \end{bmatrix},$$

$$\mathcal{R} = \begin{bmatrix} \rho & \kappa \\ \kappa^\dagger & 1 - \rho^* \end{bmatrix}, \quad \mathcal{R} = \mathcal{R}^2$$

$$h \equiv t + \Gamma \quad \quad \quad \Gamma_{ij} = \sum_{kl} \bar{v}_{ikjl} \rho_{lk} \quad \quad \Delta_{ij} = \frac{1}{2} \sum_{kl} \bar{v}_{ijkl} \kappa_{kl}$$

$$\rho_{ij} = \langle \Phi | c_j^\dagger c_i | \Phi \rangle = (V^* V^T)_{ij} \quad \quad \kappa_{ij} = \langle \Phi | c_j c_i | \Phi \rangle = (V^* U^T)_{ij}$$

# Gogny-D1S

$$\begin{aligned}
 V_{12} = & \sum_{i=1}^2 \exp \left[ -\frac{|\vec{r}_1 - \vec{r}_2|^2}{\mu_i^2} \right] \cdot (W_i + B_i \hat{P}_\sigma - H_i \hat{P}_\tau - M_i \hat{P}_\sigma \hat{P}_\tau) + \quad \text{Gauss part} \\
 & + t_3 (1 + x_0 \hat{P}_\sigma) \delta(\vec{r}_1 - \vec{r}_2) \left[ \rho \left( \frac{\vec{r}_1 + \vec{r}_2}{2} \right) \right]^\gamma + \text{density dependent part} \\
 & + i W_{LS} (\vec{\sigma}_1 + \vec{\sigma}_2) \cdot \vec{\nabla}_{12} \times \delta(\vec{r}_1 - \vec{r}_2) \vec{\nabla}_{12} + V_{\text{Coul.}}, \quad \text{L-S part}
 \end{aligned}$$

**Coulomb part is NOT included**

$$\mu_1 = 0.7 \text{ fm}$$

$$W_1 = -1720.3 \text{ MeV}$$

$$B_1 = 1300 \text{ MeV}$$

$$H_1 = -1813.53 \text{ MeV}$$

$$M_1 = 1397.60 \text{ MeV}$$

$$t_3 = 1390.60 \text{ MeV fm}^{3(1+\gamma)}$$

$$\gamma = 1/3$$

$$\mu_2 = 1.2 \text{ fm}$$

$$W_2 = 103.639 \text{ MeV}$$

$$B_2 = -163.483 \text{ MeV}$$

$$H_2 = 162.812 \text{ MeV}$$

$$M_2 = -223.934 \text{ MeV}$$

$$x_0 = 1$$

$$W_{LS} = 130 \text{ MeV fm}^5$$

- basis function : three-dimensional harmonic oscillator wave functions
- space :  $N_{shell} = n_x + n_y + n_z \leq 5$

initial conditions:

- $Q_{20}$  type impulse on ground state (impulse type)
- constrained state with quadrupole operator (constraint type)

## initial $\mathbf{U}$ & $\mathbf{V}$

$$V_k(t = 0) \rightarrow \underline{\exp(i\epsilon Q_0)} V_k(t = 0)$$

$$= \sum_{\nu} \frac{i^{\nu} \epsilon^{\nu} Q_0^{\nu}}{\nu!} V_k(t = 0)$$

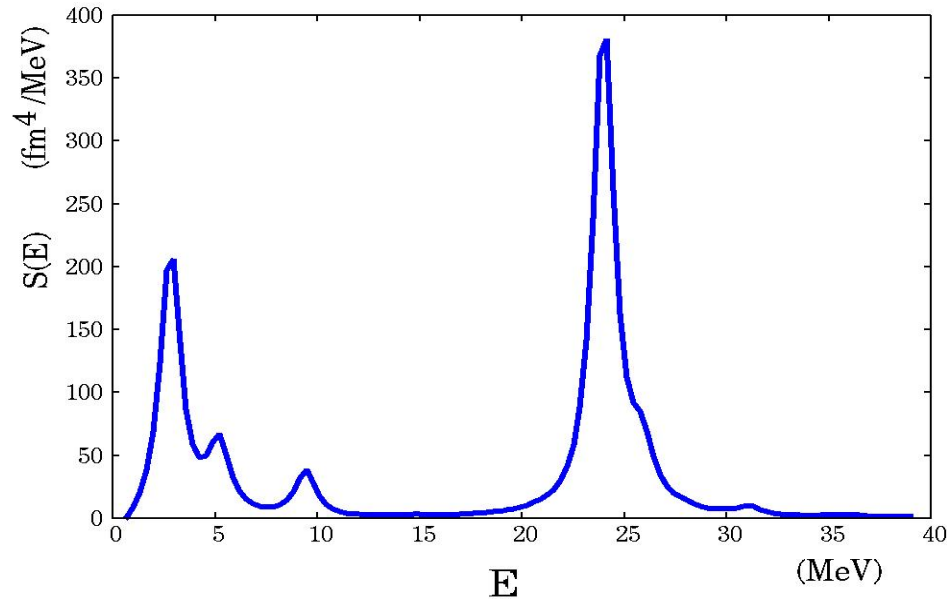
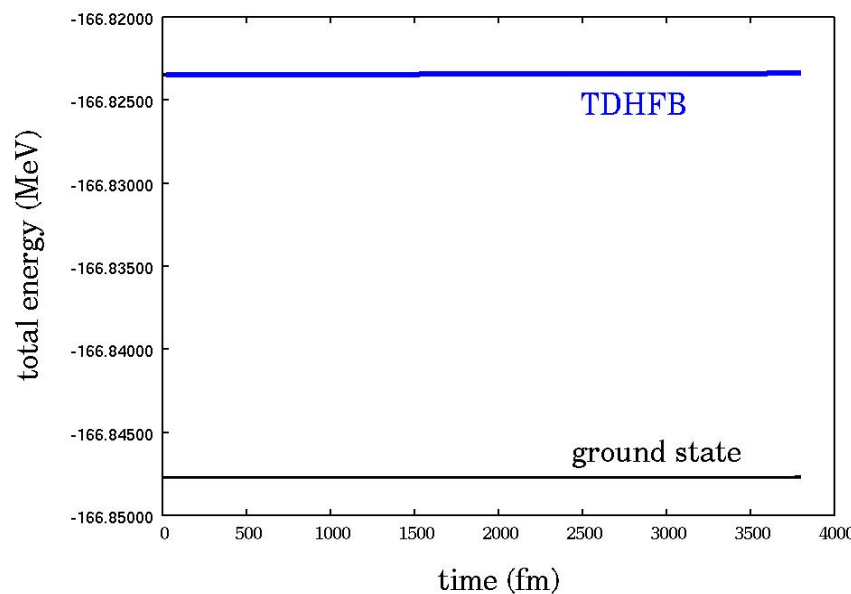
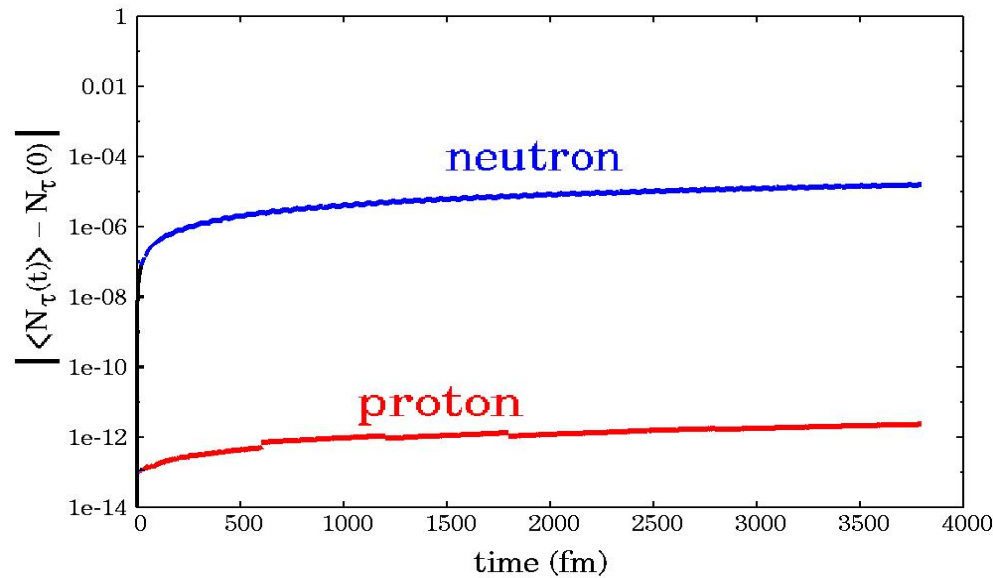
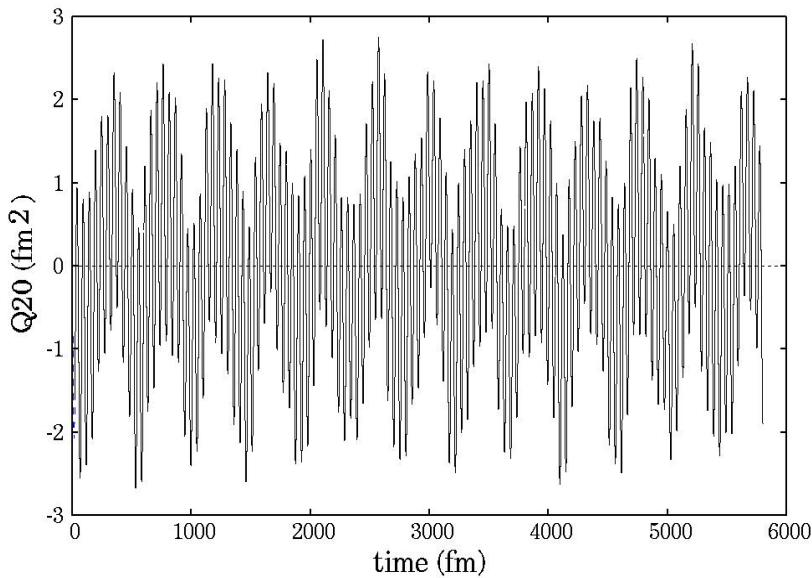
$$U_k(t = 0) \rightarrow \underline{\exp(-i\epsilon Q_0^*)} U_k(t = 0)$$

HFB ground state  $\mathbf{U}, \mathbf{V}$

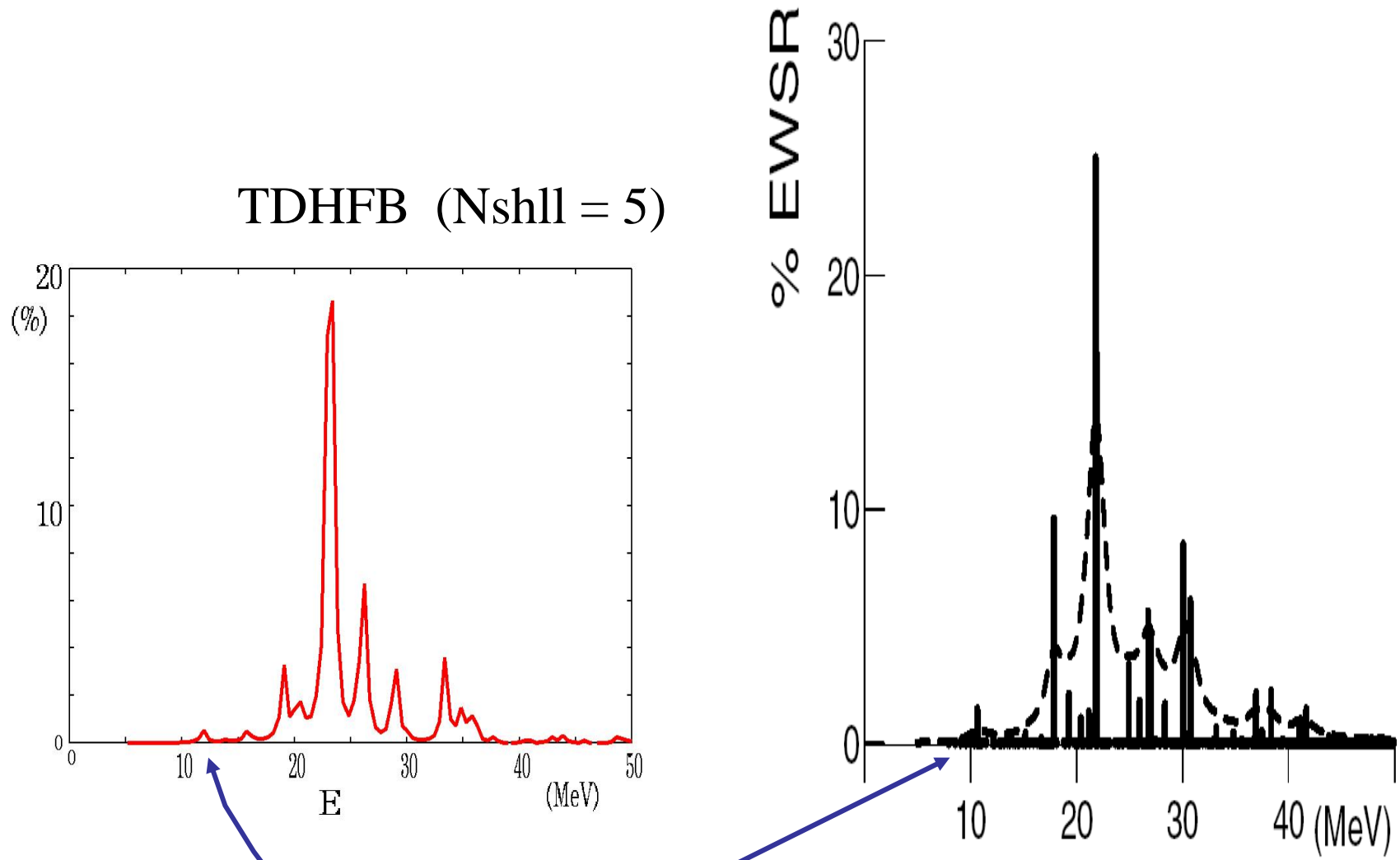
$Q_0$  : matrix representation of multipole operator

$$Q_{20} = 2z^2 - x^2 - y^2 \text{ [fm}^2]$$

# Example-1: $^{20}\text{O}$ quadrupole oscillation



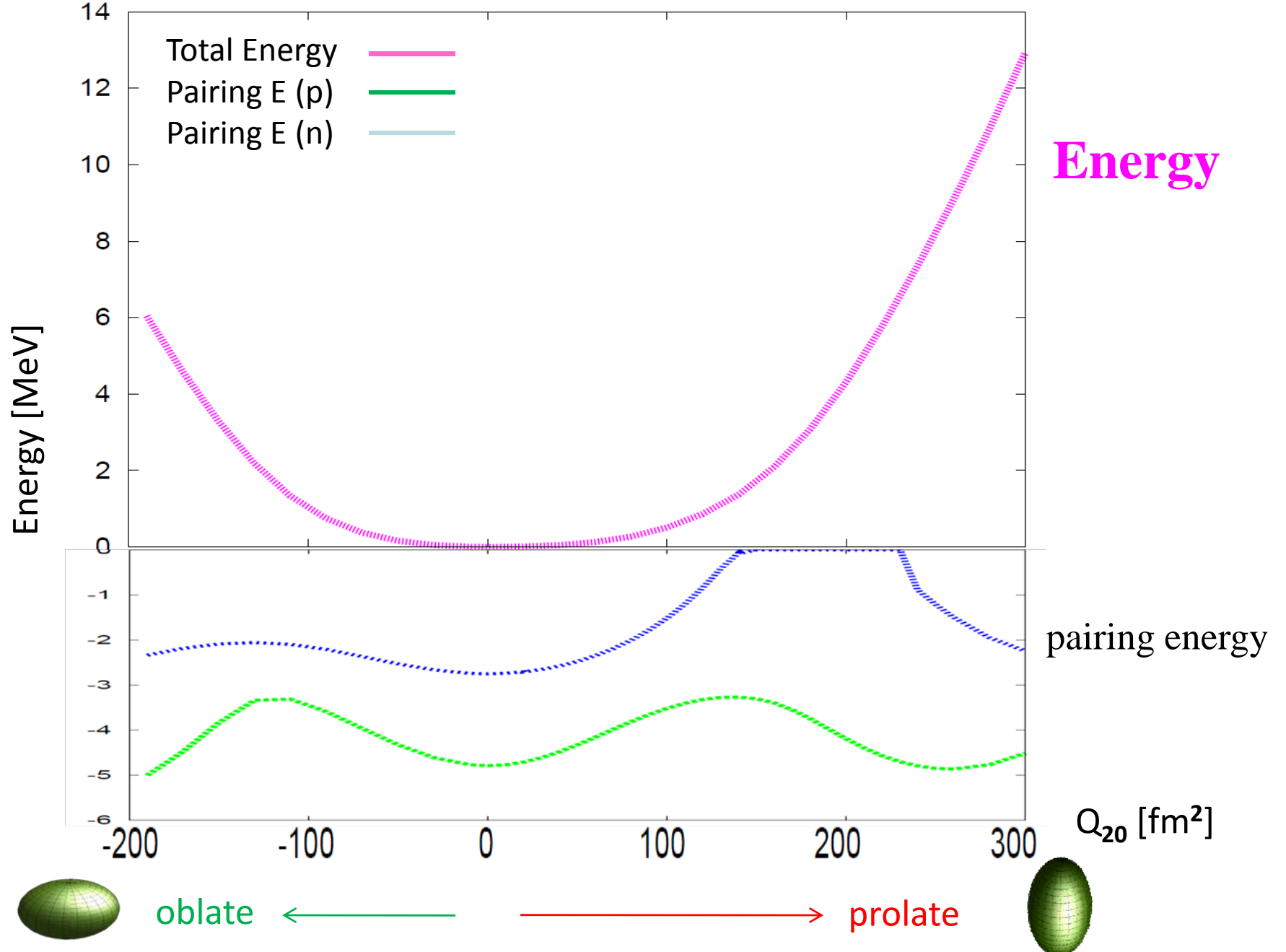
## Example-2. Spherical case: $^{26}\text{Ne}$ IV dipole response



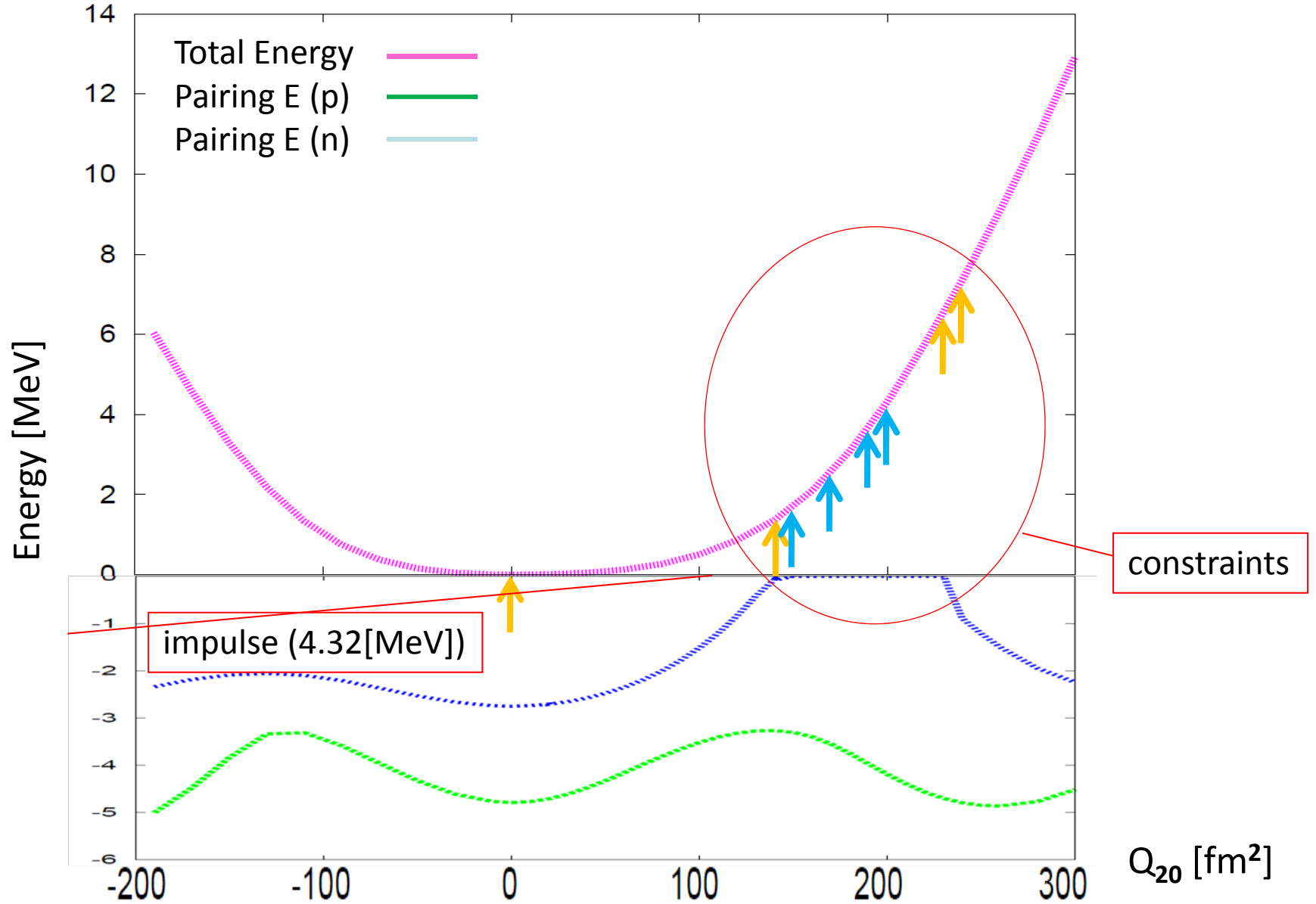
S. Peru, H. Goutte, J.F. Berger,  
Nucl. Phys. A788(2007), 44-49.

# **$^{52}\text{Ti}$ results**

- ★ Larger excitation energy
- ★ Larger amplitude ← “intermediate amplitude”



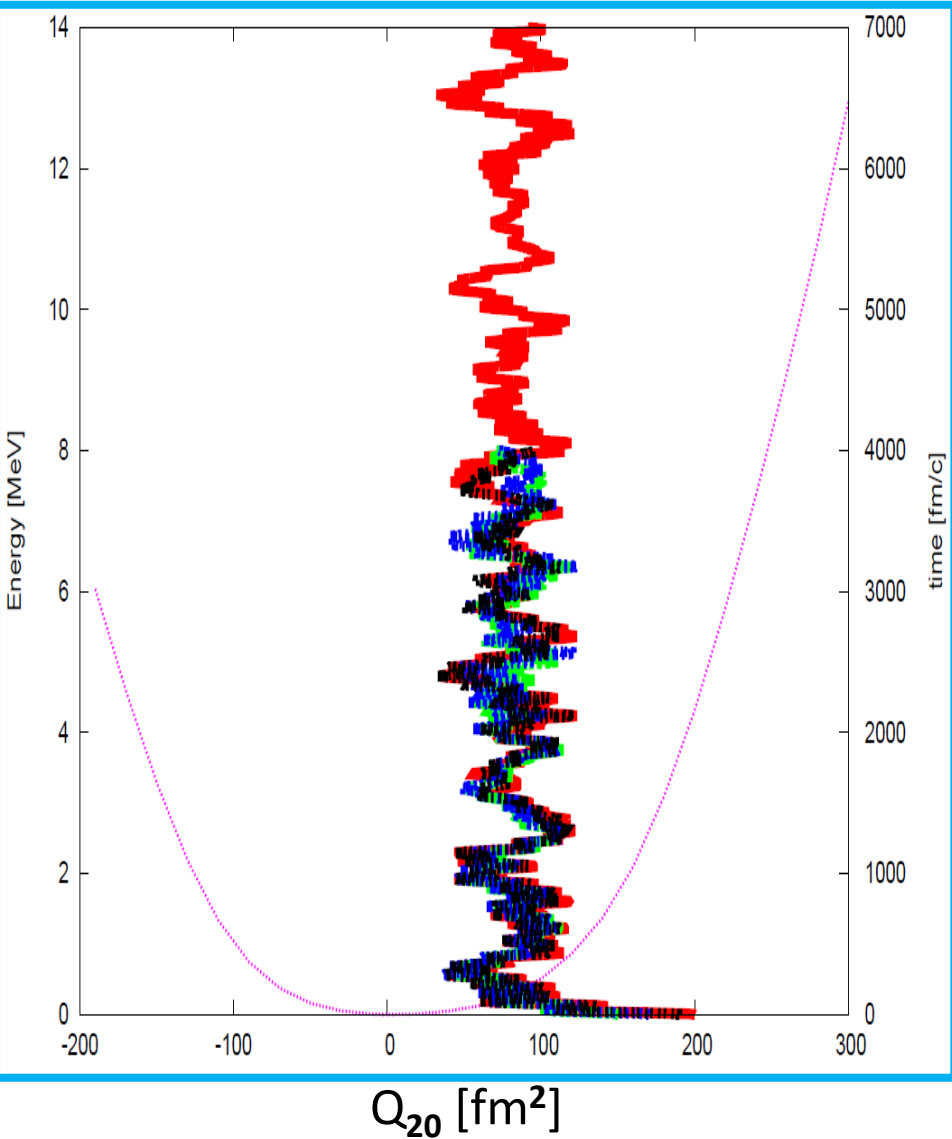
energy curve  $E$  vs  $\langle Q_{20} \rangle$  ( $^{52}\text{Ti}$  ( $Z = 22, N = 30$ )))



initial conditions

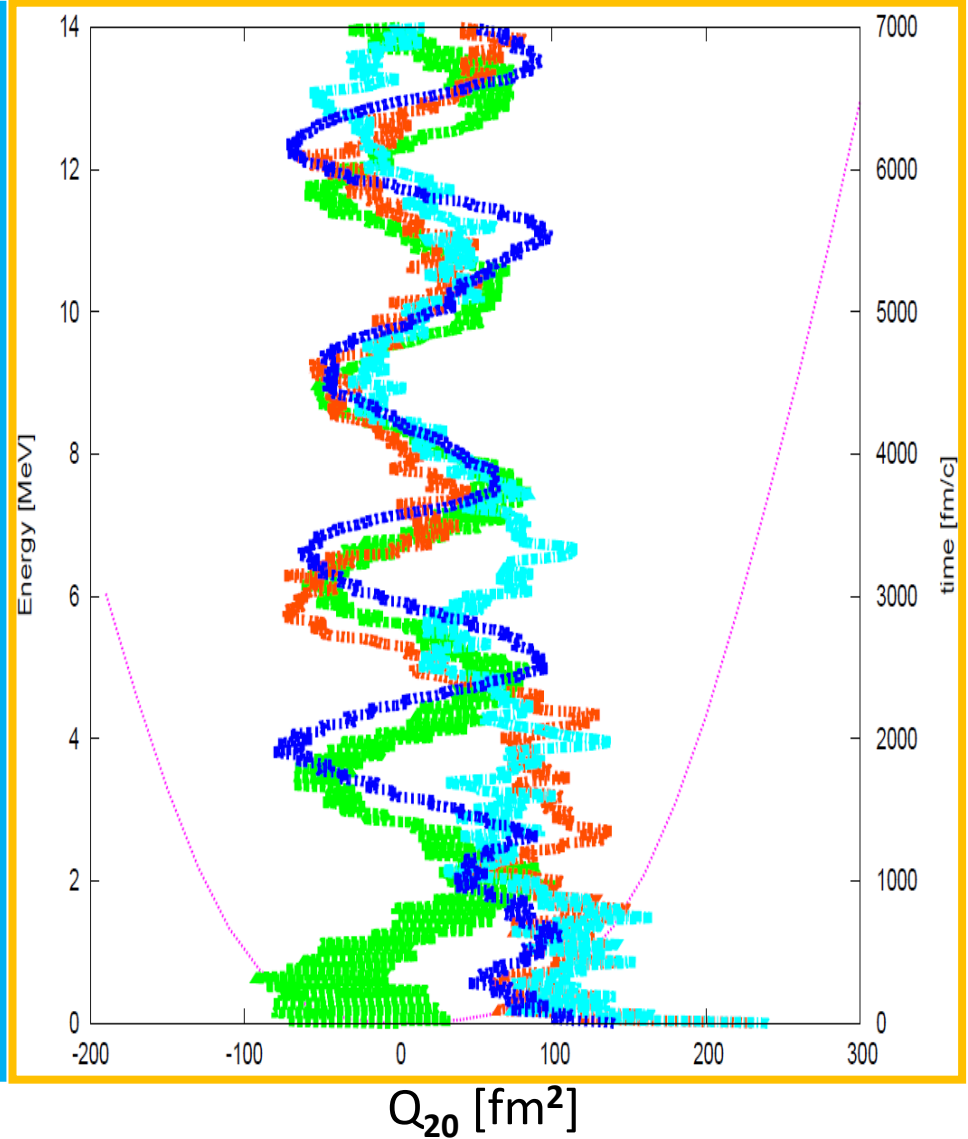
↑ ... pairing in neutrons ( impulse ,  $Q_{20} = 140 , 230 \sim 240$  [fm $^2$ ] )

↑ ... NO pairing in neutrons ( $Q_{20} = 150 \sim 200$  [fm $^2$ ] )



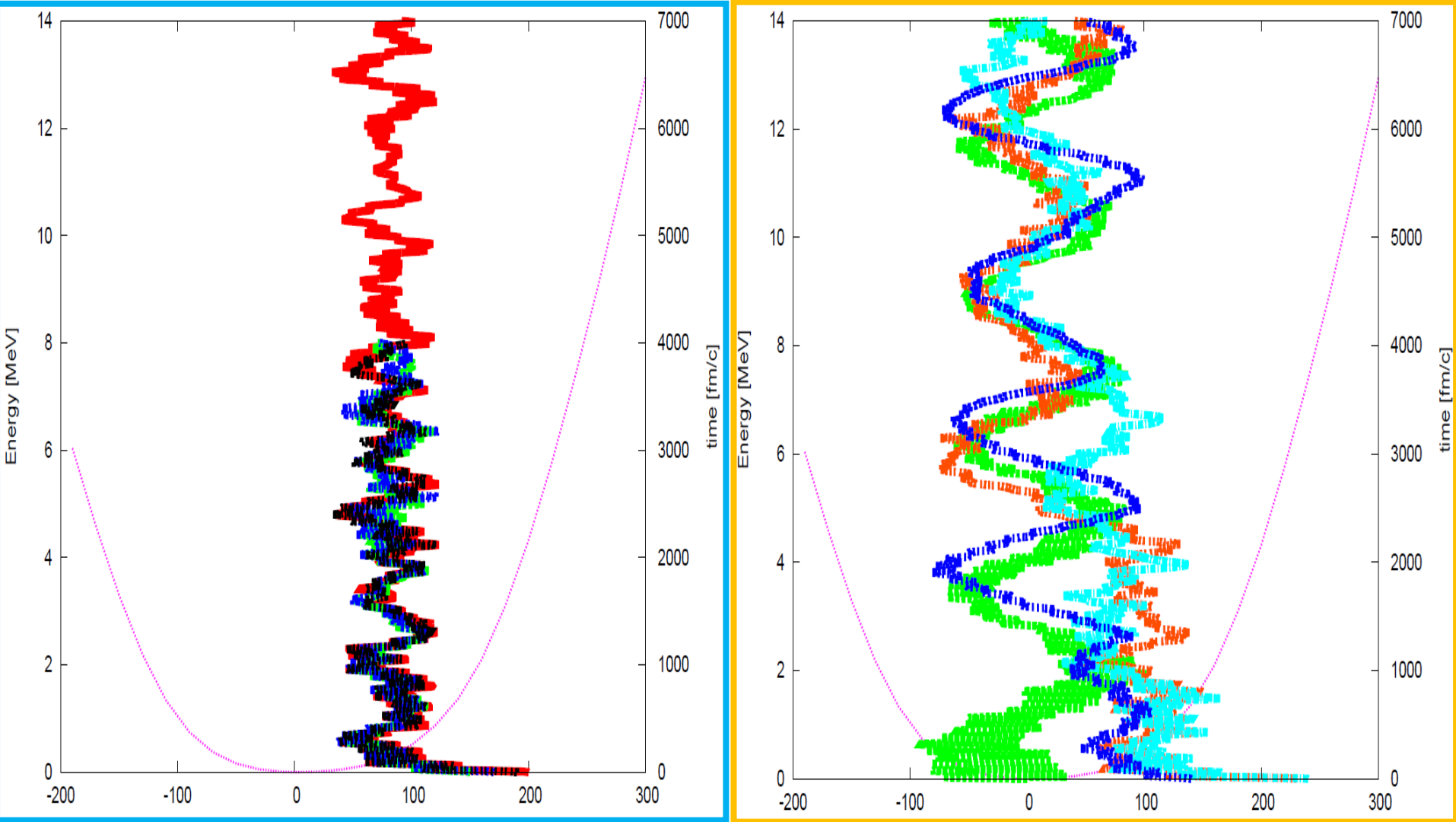
↑ ... no pairing in neutrons

oscillation around  $Q_{20} = 85 \text{ fm}^2$



↑ ... pairing in neutrons

oscillations around  $Q_{20} = 0 \text{ fm}^2$

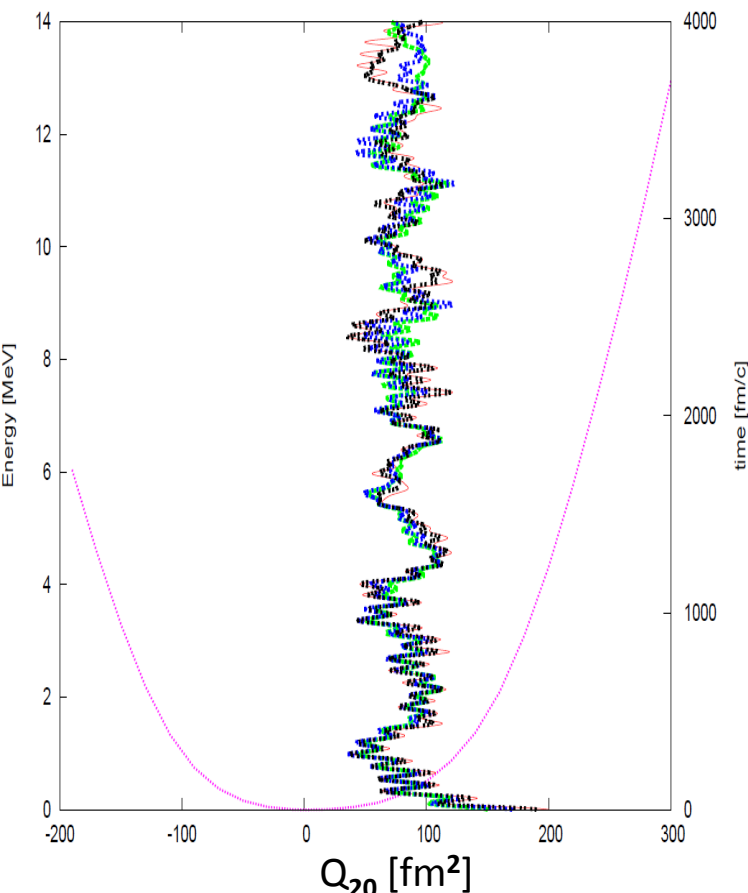


- two types of oscillations after relaxation process
- effects of pairing correlations in oscillating motions

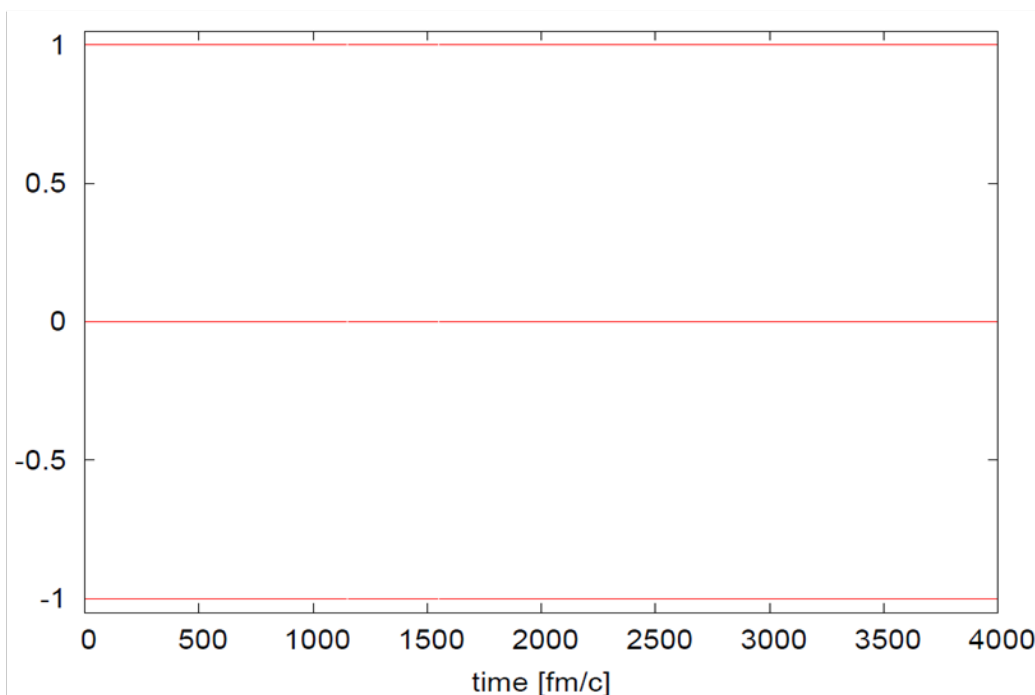
→ put focus on the occupation probabilities of TDHFB orbitals

$$\sum_i V_{ij}^* V_{ij}$$

# Case 1: oscillations around $Q_{20} = 85 \text{ [fm}^2\text{]}$ (constraint $Q_{20} = 170 \text{ [fm}^2\text{]}$ )



time dependence  
of occupation probability (neutrons)



initial condition :  $Q_{20} = 170 \text{ [fm}^2\text{]}$

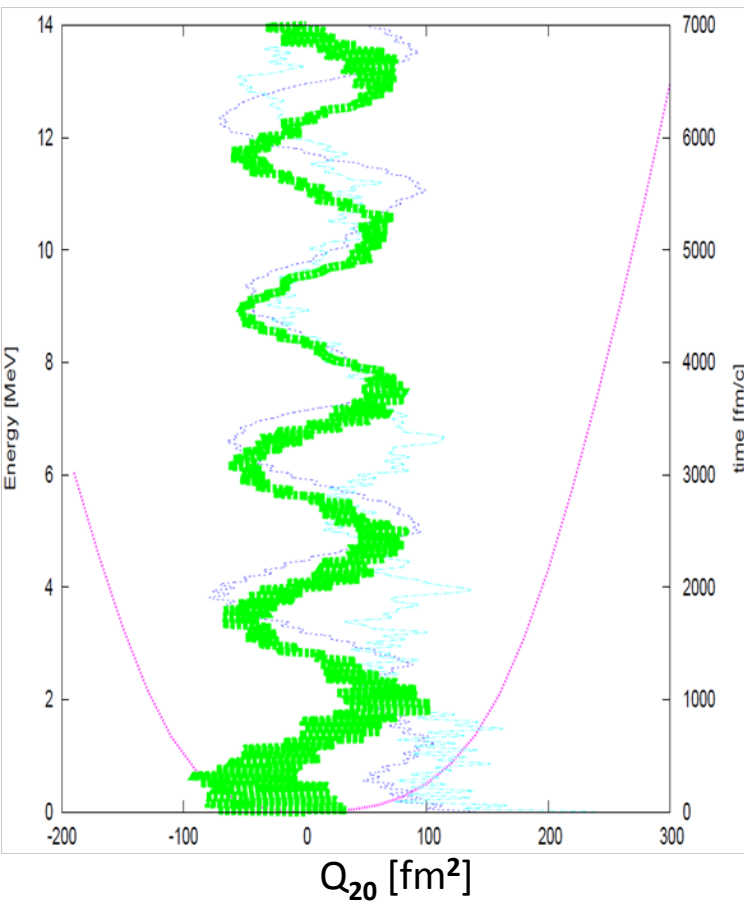
$E_x = 2.56 \text{ [MeV]}$

$E_{\text{pair}}(\text{proton}) = -3.55 \text{ [MeV]}$

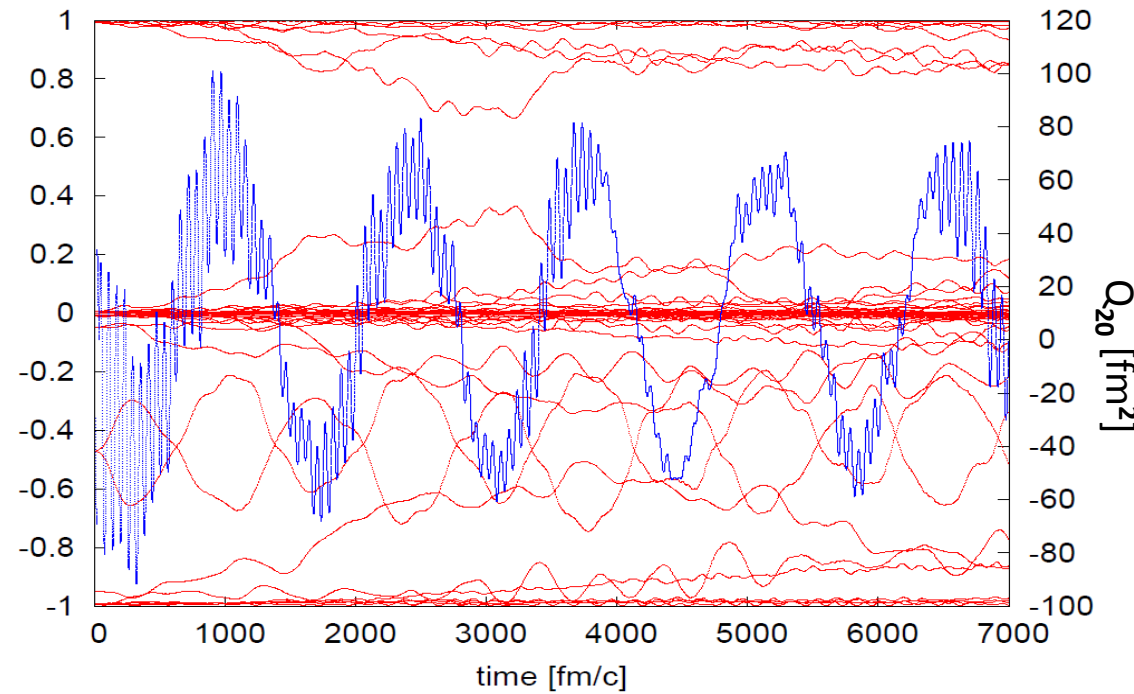
$E_{\text{pair}}(\text{neutron}) = 0 \text{ [MeV]}$

- no pairing in neutrons  
→ no jump into ground state pocket ( $Q_{20} = 0 \text{ [fm}^2\text{]}$ )

## Case 2: oscillations around ground state ( $Q_{20} = 0$ [fm $^2$ ] ) (impulse type)



time dependence  
of occupation probability (neutrons)



impulse type

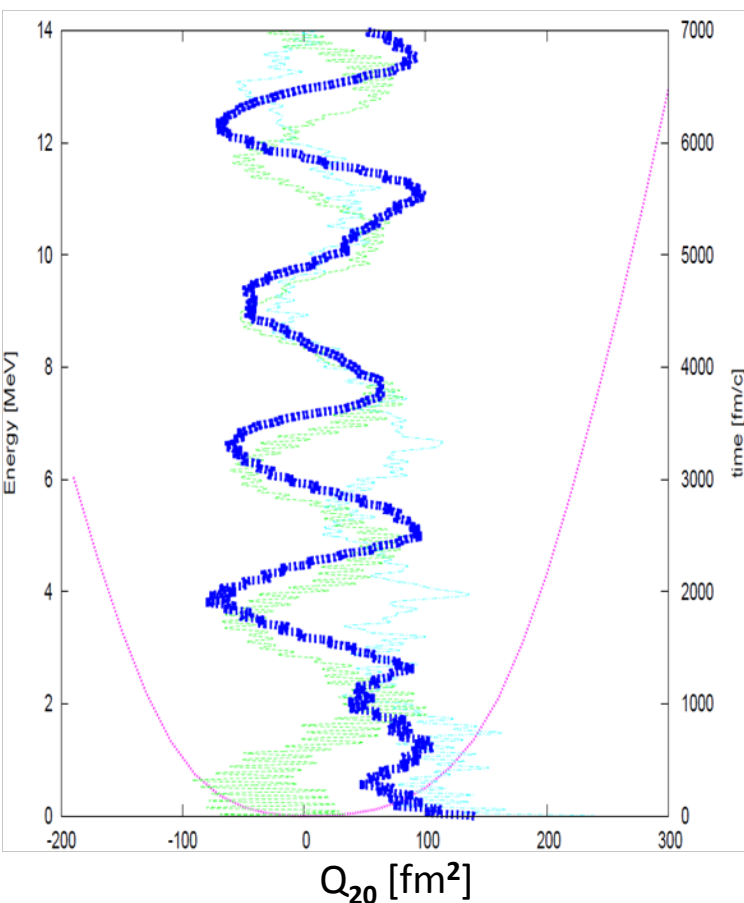
$$E_x = 4.32 \text{ [MeV]}$$

$$E_{\text{pair(proton)}} = -4.79 \text{ [MeV]}$$

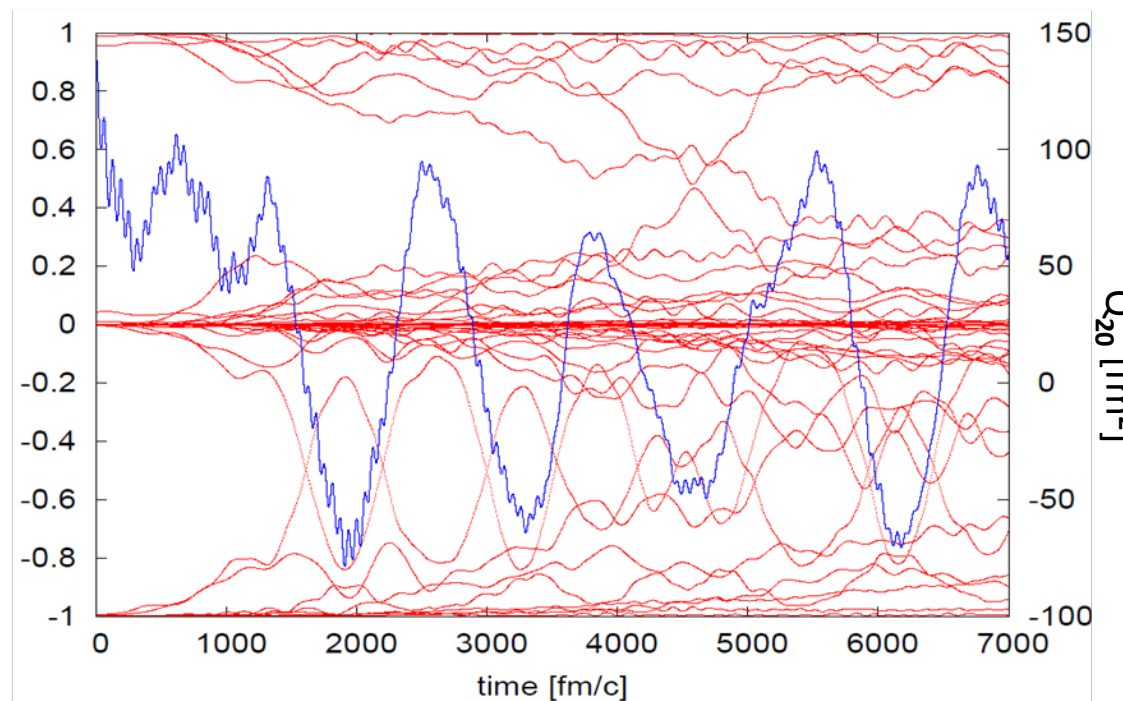
$$E_{\text{pair(neutron)}} = -2.75 \text{ [MeV]}$$

- two main trajectories
- $Q_{20}$  oscillation  $\leftrightarrow$  seesaw in occupation probabilities

# Case 3: jump into ground state pocket (constraint $Q_{20} = 140 \text{ [fm}^2\text{]}$ )



time dependence  
of occupation probability (neutrons)



initial condition :  $Q_{20} = 140 \text{ [fm}^2\text{]}$

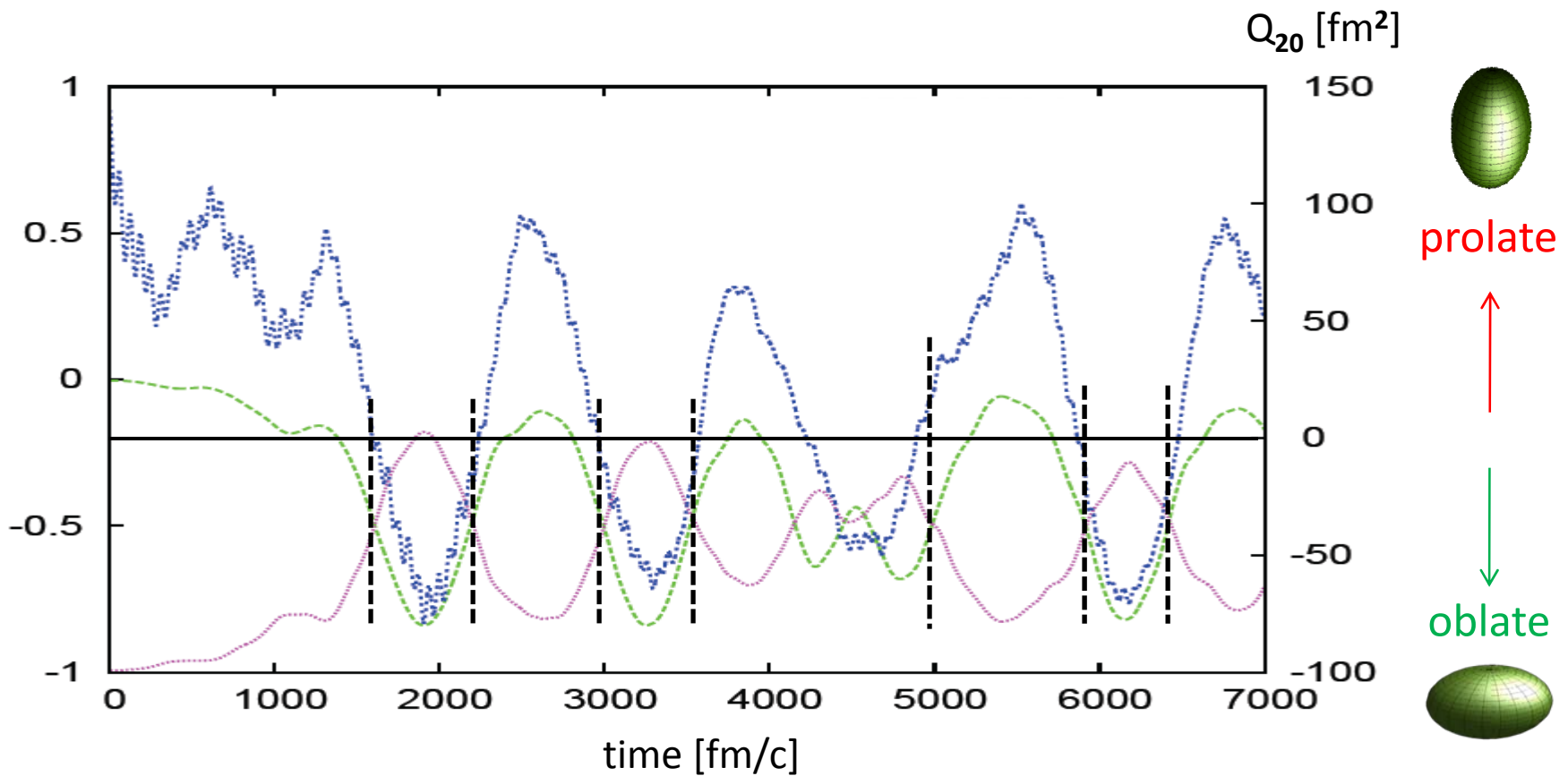
$E_x = 1.37 \text{ [MeV]}$

$E_{\text{pair(proton)}} = -3.27 \text{ [MeV]}$

$E_{\text{pair(neutron)}} = -0.07 \text{ [MeV]}$

- sudden change in occupation probability  
→  $Q_{20}$  oscillation jumps
- characteristic two orbitals
- in phase with  $Q_{20}$  oscillation

variations of occupation probabilities of  
two main trajectories (constraint  $Q_{20} = 140$  [fm $^2$ ])



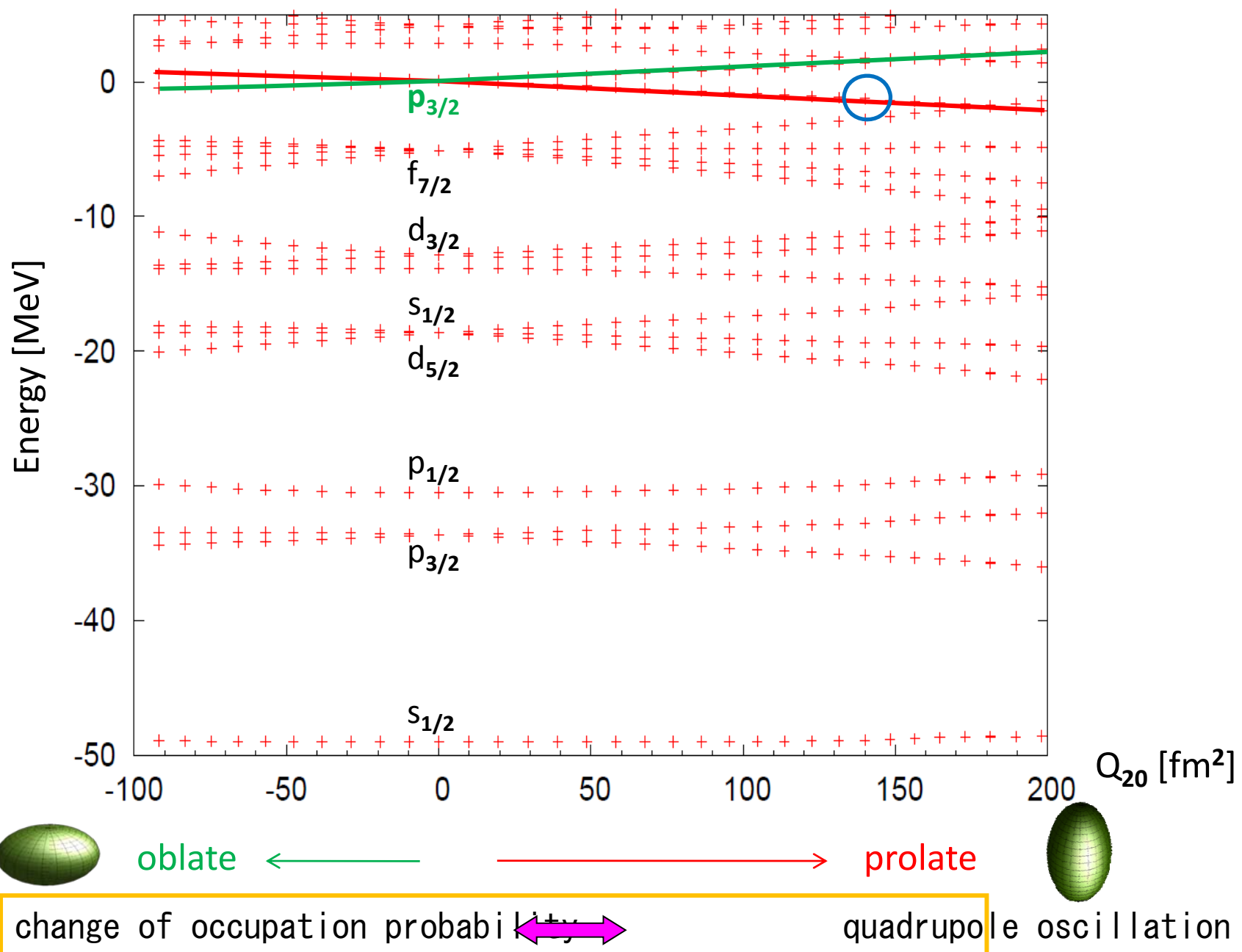
prolate side ... red orbital main

$$(n_x, n_y, n_z) = (3, 0, 0)$$

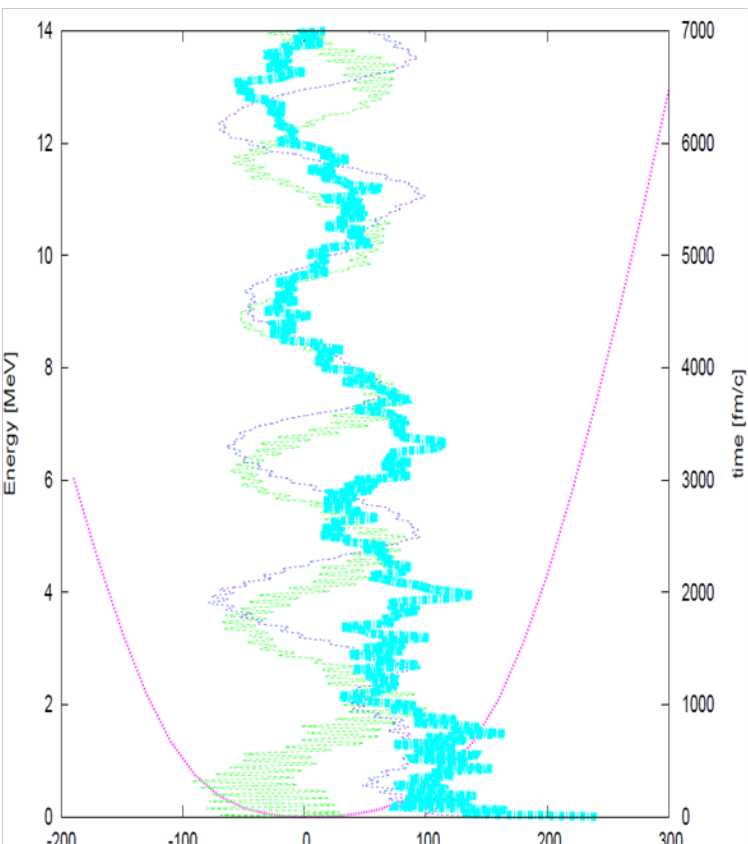
oblate phase ... green orbital main

$$(n_x, n_y, n_z) = (0, 3, 0), (0, 0, 3)$$

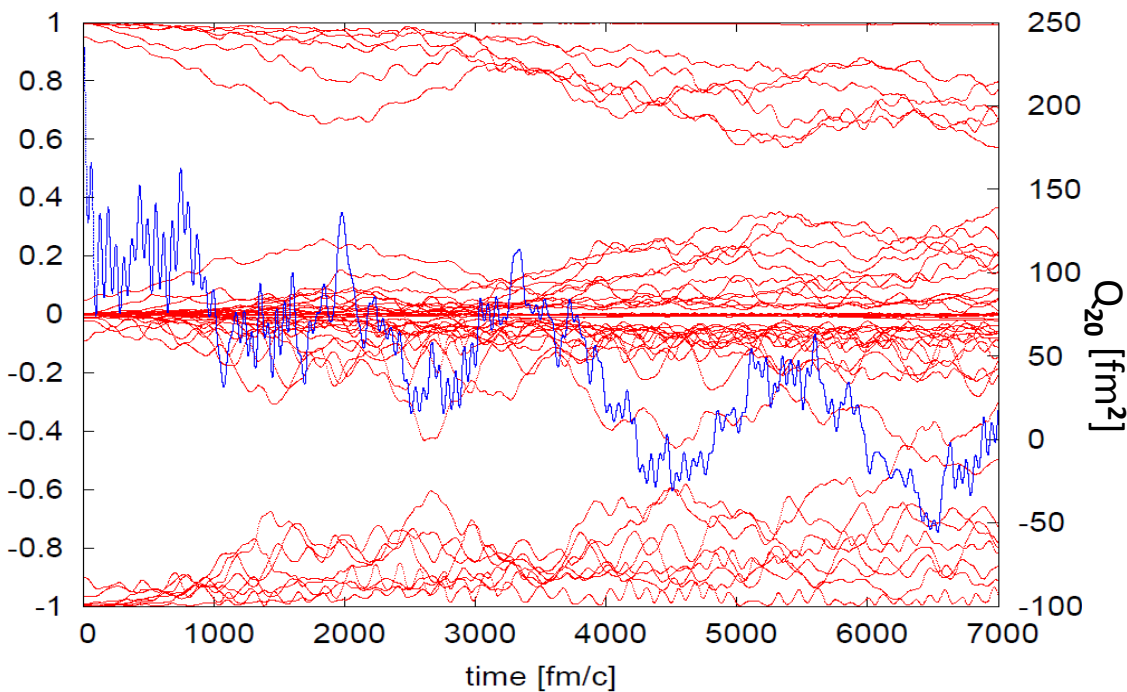
# $^{52}\text{Ti}$ ( $Z = 22$ , $N = 30$ ) one particle levels (neutrons)



# Case 4: slow relaxation (constraint $Q_{20} = 240$ [fm $^2$ ])



準粒子軌道の占有率の時間変化（中性子）



initial condition :  $Q_{20} = 240$  [fm $^2$ ]

$E_x = 7.37$  [MeV]

$E_{\text{pair}}(\text{proton}) = -4.79$  [MeV]

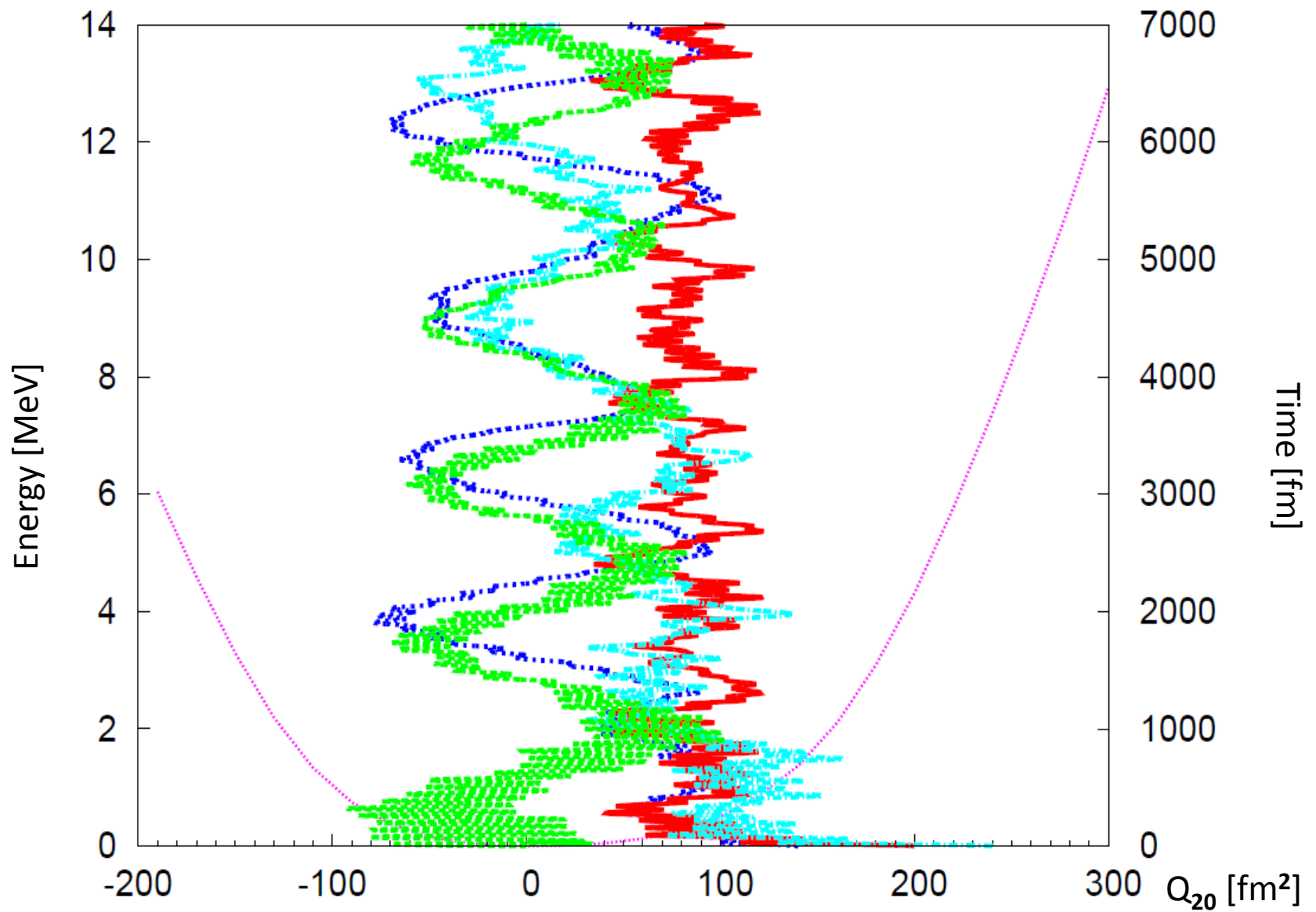
$E_{\text{pair}}(\text{neutron}) = -0.89$  [MeV]

## slow relaxation

- occupation probabilities of many orbitals change  
→ two main orbitals becomes unclear

period → OK

unsolved problem: **amplitudes**



Impulse type

Ex E= 4.32[MeV]  
Pairing E (p)= -4.79[MeV]  
Pairing E (n)= -2.75[MeV]

Initial  $Q_{20} = 140$

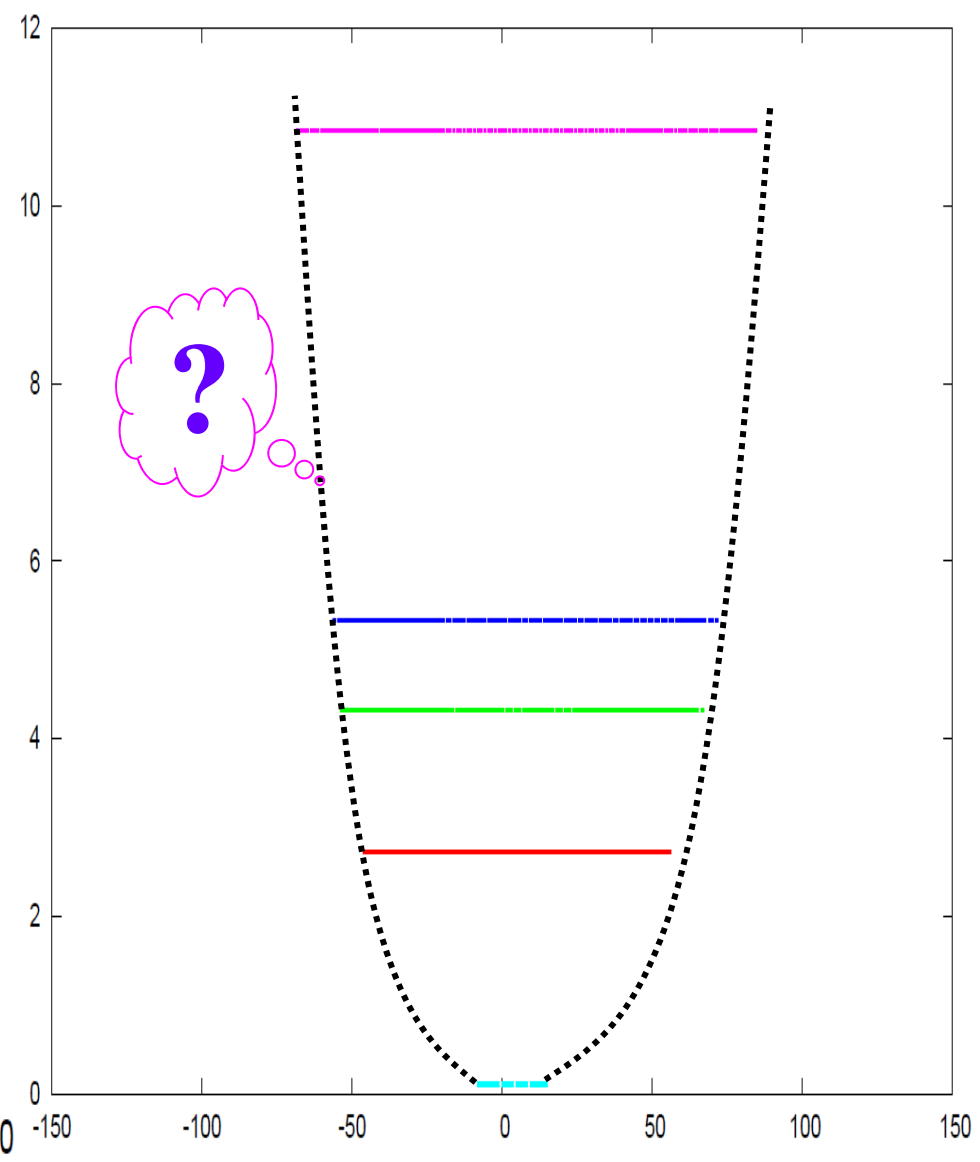
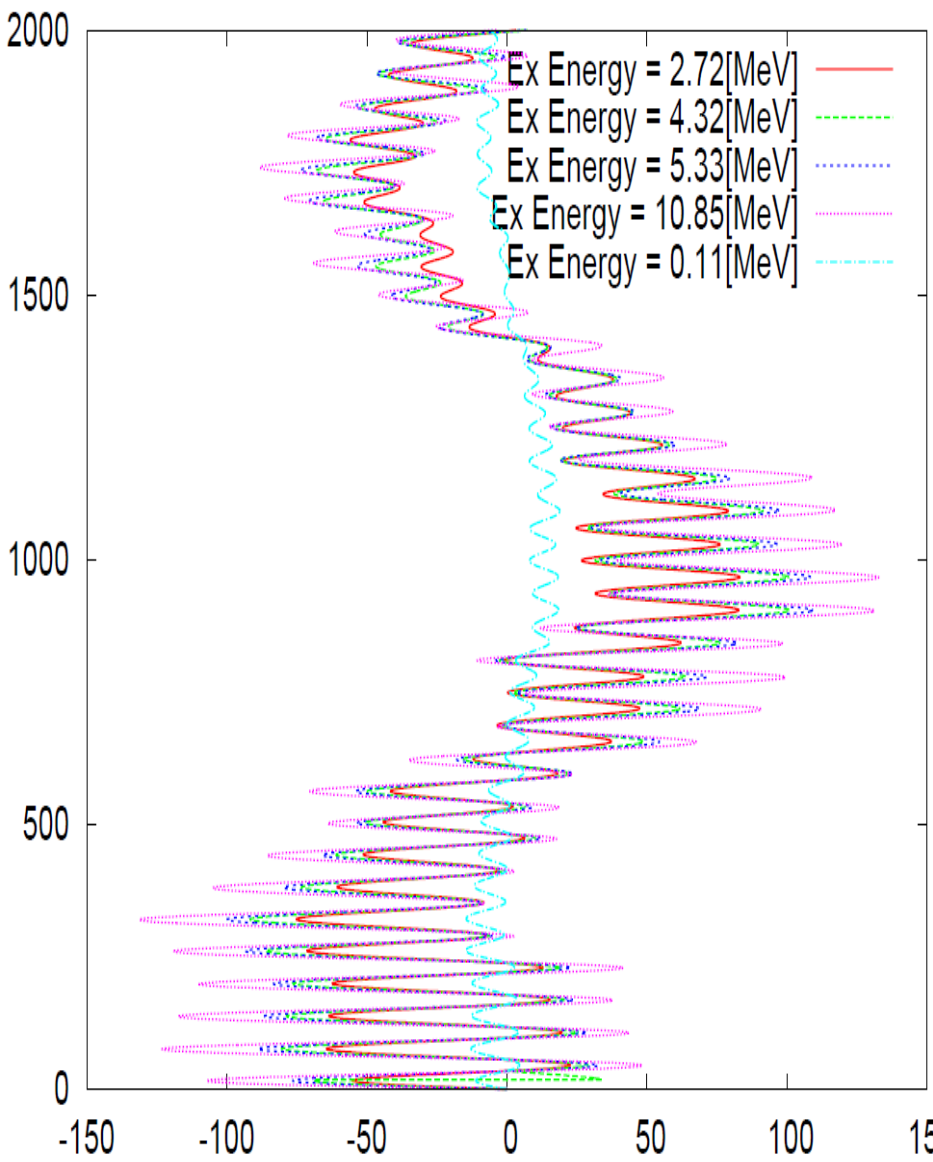
Ex E= 1.37[MeV]  
Pairing E (p)= -3.27[MeV]  
Pairing E (n)= -0.07[MeV]

Initial  $Q_{20} = 200$

Ex E=4.32 [MeV]  
Pairing E (p)= -4.19[MeV]  
**Pairing E (n)=0 [MeV]**

Initial  $Q_{20} = 240$

Ex E= 7.37[MeV]  
Pairing E (p)= -4.79[MeV]  
Pairing E (n)= -0.89[MeV]



Amplitudes of slow oscillations with excitation energy from 2.72 to 10.85 [MeV]  
vary very slowly.

# Summary

1. Intermediate amplitude collective oscillations are calculated in terms of TDHFB with Gogny interaction.
2. Pairing correlation easily affects the oscillations:
  - \* center of oscillation
  - \* period, amplitude
  - \* relaxation time
3. occupation probability changes continuously  
     $\leftrightarrow$  quantum numbers are discrete  
    Oscillation with long period may easily come out.
4. improvements in future :
  - \* better basis
    - Gogny TDHFB with **GEM**, **cylindrical** HO basis, .....
  - \* connections with microscopic analysis such as **AdSCC**.